

# Limits on the parameters of the equation of state for interacting dark energy

Germán Izquierdo<sup>1</sup> and Diego Pavón<sup>2</sup>

<sup>1</sup>*Institut de Mathématiques de Bourgogne, Université de Bourgogne,  
9 Av. Alain Savary, 21078 Dijon Cedex, France*

<sup>2</sup>*Departamento de Física, Universidad Autónoma de Barcelona,  
08193 Bellaterra (Barcelona), Spain*

## Abstract

Under the assumption that cold dark matter and dark energy interact with each other through a small coupling term,  $Q$ , we constrain the parameter space of the equation of state  $w$  of those dark energy fields whose variation of the field since last scattering do not exceed Planck's mass. We use three parameterizations of  $w$  and two different expressions for  $Q$ . Our work extends previous ones.

## I. INTRODUCTION

The equation of state parameter of dark energy -the mysterious agent responsible for the current accelerated expansion of the Universe- ranks among the biggest unknowns in cosmology. It is usually written as  $w = p_\phi/\rho_\phi$  and lies in the range  $(-1, -1/3)$  if the dark energy is quintessence, and  $(-\infty, -1)$  if it is of phantom type; in either case it may run with expansion. By contrast, in the very particular (but observationally favored) instance of a cosmological constant  $w$  stays fixed at  $-1$ . It is then apparent that some knowledge on the nature of dark energy can be gained by setting limits on  $w$ .

Observational constraints on this quantity from supernovae type Ia (SN Ia), temperature anisotropies of the cosmic microwave background radiation (CMB), baryon acoustic oscillations (BAO), etc, suggest that nowadays  $w$  is not far from the cosmological constant value. However, all these studies rest on some or other world model and on inevitable priors imposed upon the parameters space to ease the data analysis.

Recently, bounds on  $w$  have been derived from the very reasonable requirement that the variation experienced by the dark energy scalar field  $\phi$  (regardless it may be phantom or quintessence) from any redshift,  $z$ , within the classical expansion era, till now should not exceed Planck's mass (see Huang [1], and Saridakis [2]). This is to say

$$|\Delta\phi(z)|/M_P < 1, \quad (1)$$

where -as can be readily deduced-

$$\frac{|\Delta\phi(z)|}{M_P} = \frac{1}{M_P} \int_t^{t_0} \dot{\phi} dt = \int_0^z \frac{\sqrt{3|1+w(x)|\Omega_\phi(x)}}{1+x} dx. \quad (2)$$

Huang's analysis confines itself to quintessence fields with various  $w$  parameterizations (viz:  $w$  constant, a linear function of redshift, and the Chevallier-Polarski-Linder parametrization [3, 4]) [1]. Saridakis considers phantom fields only and uses identical parameterizations than Huang plus a further one in which  $w$  depends linearly on the logarithm of the scale factor [2].

The bound (1) looks a rather natural condition and persuasive arguments have been advanced in its favor [5–7]. Moreover, we have found a further, solid, motivation for it. Namely: if condition (1) is violated, then dark energy dominates at very early times which cannot be reconciled with observation (see Fig. 4 and “forbidden” regions on the top right

corner of the panels of figures 6, 9, and 11, below). In particular, as noted by Bean *et al.* [8], the fractional density of dark energy cannot exceed 5% and 39% at the primeval nucleosynthesis and recombination epochs, respectively, -we shall elaborate on this in a future publication. Nevertheless, we refrain ourselves from imposing (1) on every dark energy field. Its seems safer to demand that  $|\Delta\phi|/M_P$  be not much larger than order unity. However, the latter requirement cannot be easily implemented and, at any rate, it would translate on rather loose constraints on  $w$ . Therefore, we choose to circumscribe our analysis to dark energy fields that fulfill condition (1).

In Huang's as well as in Saridakis' work matter and dark energy interact with each other only gravitationally. Certainly this is a reasonable assumption but nonetheless minimalist since, while dark energy interactions with baryons are severely restricted by solar system experiments [9], there is nothing against a possible coupling (interaction) with dark matter. On the contrary, a transfer from dark energy to dark matter alleviates the cosmic coincidence problem (the observational fact that both energy densities are comparable today [10]) and may solve it in full [11]. Besides, as revealed by optical, x-ray and weak-lensing data, the internal dynamics of 33 relaxed galaxy clusters seems to favor such interaction [12]. Likewise, a recent analysis using the 397 SN Ia of the "Constitution" set [13], BAO and CMB data adds significant weight to the existence of the coupling [14]. In fact, the subject has evolved into a field of active research -see e.g. [15, 16] and references therein; a recent review can be found in [17].

In the presence of a coupling, say  $Q$ , the continuity equations for the three main contributors to the present cosmic budget adopt the form,

$$\begin{aligned}\dot{\rho}_b + 3H\rho_b &= 0, \\ \dot{\rho}_c + 3H\rho_c &= Q, \\ \dot{\rho}_\phi + 3H(1+w)\rho_\phi &= -Q,\end{aligned}\tag{3}$$

where the subscripts,  $b$ ,  $c$ , and  $\phi$  stands for baryons, cold dark matter, and dark energy, respectively. This paper aims to constrain different parameterizations of  $w$  under diverse expressions for  $Q$ . Regrettably, guidelines about the latter are rather loose: it must be positive-semidefinite and small. If  $Q$  were negative, the energy densities could become negative, and the second law of thermodynamics get violated [18]. If it were large, dark energy would have dominated the expansion at early times and possibly not today. Thus,

for the time being, we must content ourselves with guessing plausible expressions for  $Q$  just on phenomenological bases.

In view of the above equations the coupling must be a function of  $H\rho_c$  and  $H\rho_\phi$ . By power law expanding it up to first order on these quantities we write  $Q(H\rho_c, H\rho_\phi) \simeq \epsilon_c H\rho_c + \epsilon_\phi H\rho_\phi$ , where both  $\epsilon$  coefficients ought to be non-negative and small (i.e., not larger than, say,  $10^{-1}$ ). To simplify the analysis we will consider in turn that one of the two coefficients vanishes. So, we will take

$$Q = 3\epsilon H\rho_\phi, \quad \text{and} \quad Q = 3\epsilon H\rho_c, \quad (4)$$

-the factor 3 being introduced for mathematical convenience.

At this point one may object that if  $Q$  is small, no significant difference with the results of Huang [1] and Saridakis [2] should be expected. However, as we shall see, this is not the case. *A priori* we can argue in favor of some non small departure from the findings of [1] and [2] by considering the ratio between  $Q$  and the second term in last equation of (3). Indeed, dividing the right hand side of (4.1) by the second term of the said equation yields  $\epsilon/(1+w)$ . In general, this ratio cannot be neglected and it can be large in absolute value when  $w$  is close to  $-1$ . Likewise, using instead (4.2) we have  $\epsilon\rho_c/(1+w)\rho_\phi$ . Its absolute value can be of order unity, or even larger, for extended periods of the cosmic history.

Although expressions (4) were proposed on phenomenological grounds they can be obtained in scalar-tensor gravity from the action (in the Einstein frame) [19]

$$S = \int d^4x \sqrt{-g} \left\{ \frac{1}{16\pi G} R - \frac{1}{2} \partial_a \phi \partial^a \phi + \frac{1}{\chi^2(\phi)} L_c(\zeta, \partial\zeta, \chi^{-1} g_{ab}) + L_b(\xi, \partial\xi, \chi^{-1} g_{ab}) \right\}. \quad (5)$$

Here  $R$  denotes the Ricci scalar,  $L_c$  and  $\zeta$  stand for the dark matter Lagrangian and the dark matter degrees of freedom, respectively (corresponding meanings have  $L_b$  and  $\xi$ ); on the other hand,  $\chi(\phi)$  couples dark matter with the dark energy field  $\phi$ . From (5) the interaction term between dark matter and dark energy can be expressed as

$$Q = H\rho_c \left[ \frac{d(\ln \bar{\chi}(a))}{d \ln a} \right], \quad (6)$$

where  $\bar{\chi}(a) = \chi(a)^{(3w_c-1)/2}$  with  $w_c$  the equation of state parameter of dark matter (zero in our case). By choosing

$$\bar{\chi}(a) = \bar{\chi}_0 \exp \left[ 3 \int \frac{\epsilon_\zeta \rho_\zeta + \epsilon_c \rho_c}{\rho_c} d \ln a \right], \quad (7)$$

the first (second) expressions for  $Q$  in (4) follows after using (6) and setting  $\epsilon_c = 0$  ( $\epsilon_\zeta = 0$ ). Similar expressions for  $Q$  have been obtained from the above action in Refs. [20] and [21].

In this paper we shall assume a spatially flat Friedmann-Robertson-Walker universe with present fractional densities of baryons and cold dark mater  $\Omega_{b0} = 0.04$ , and  $\Omega_{c0} = 0.24$ , respectively, throughout. As usual, a zero subindex means the current value of the corresponding quantity; likewise we normalize the scale factor of the metric by setting  $a_0 = 1$ .

## II. INTERACTION TERM PROPORTIONAL TO THE DARK ENERGY DENSITY

In this section we consider  $Q = 3\epsilon H\rho_\phi$  alongside different expressions for the equation of state parameter.

### A. Constant $w$

By plugging  $Q = 3H\epsilon\rho_\phi$  into (3), assuming  $w = w_0$ , and integrating we get the energy densities dependence on the scale factor

$$\begin{aligned}\rho_b &= \rho_{b0} a^{-3}, \\ \rho_c &= \rho_{c0} a^{-3} + \frac{\epsilon}{w_0 + \epsilon} \rho_{\phi0} a^{-3} [1 - a^{-3(w_0 + \epsilon)}], \\ \rho_\phi &= \rho_{\phi0} a^{-3(1+w_0+\epsilon)}.\end{aligned}\tag{8}$$

We then introduce  $\Omega_\phi = \rho_\phi / (\rho_b + \rho_c + \rho_\phi)$  in (2) and numerically determine  $|\Delta\phi|/M_P$  in the redshift interval between the last scattering ( $z_{ls} = 1089$ ) and now ( $z = 0$ ) -bear in mind that  $1 + z = a^{-1}$ . Figure 1 shows  $|\Delta\phi|/M_P$  vs.  $w_0$  for different values of the parameter  $\epsilon$ . When  $-1 < w_0 < -1/3$  (left panel), for every  $\epsilon$  value there is a range of  $w_0$  that violates condition (1); the bigger the interaction strength, the bigger the  $|w_0|$  that violates the condition. By contrast, when  $w_0 < -1$  (right panel) the bound (1) is fulfilled no matter the value of  $\epsilon$ . This could have been anticipated since, in this simple case, Eq. (3.2) can be written as  $\dot{\rho}_\phi + 3H(1 + w_{eff})\rho_\phi = 0$ , i.e., as though it were no interaction but with  $w$  replaced by the effective equation of state parameter  $w_{eff} = w + \epsilon$ . At any rate, our results corroborate and extend Huang's and Saridakis'.

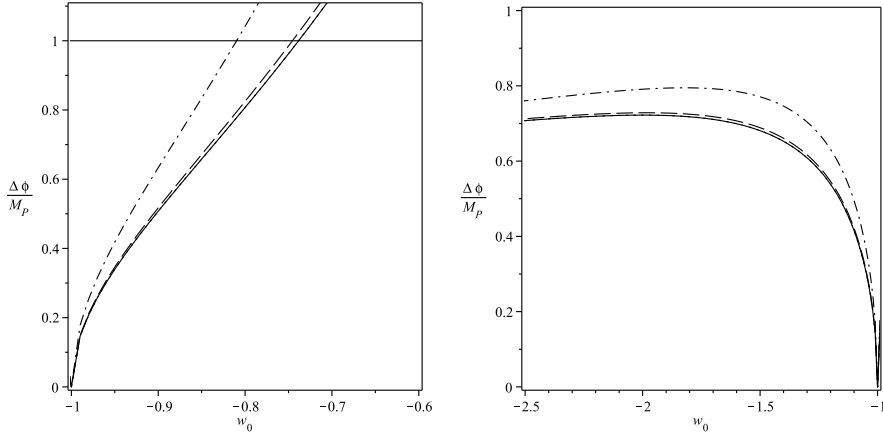


FIG. 1:  $|\Delta\phi|/M_P$  vs.  $w_0$  for  $Q$  given by (4.1) and constant  $w$  evaluated in the redshift range  $(0, 1089)$ . Left Panel: Quintessence solutions  $(-1 < w_0 < -1/3)$ . Right panel: Phantom solutions  $(w_0 < -1)$ . In both panels solid, dotted, dashed, and dot-dashed lines correspond to  $\epsilon = 0, 10^{-4}, 10^{-2}$ , and  $0.1$ , respectively. (Solid and dotted lines practically overlap). Condition (1) for  $\epsilon = 0, 10^{-4}, 10^{-2}$ , and  $0.1$  implies  $w_0 < -0.738, -0.738, -0.745$ , and  $-0.810$ , respectively. In drawing these and all subsequent figures we assumed  $\Omega_{b0} = 0.04$ , and  $\Omega_{c0} = 0.24$ .

### B. Chevallier-Polarski-Linder parametrization

Except when dark energy is given by the quantum vacuum, there is no compelling motivation to assume  $w$  constant for the whole cosmic evolution. However, its simplest generalization in terms of redshift,  $w(z) = w_0 + w_1 z$ , is not compatible with observation for it diverges as  $z \rightarrow \infty$ . This prompted the introduction of the more suitable expression  $w(z) = w_0 + w_1 \frac{z}{1+z}$  or, equivalently, in terms of the scale factor

$$w(a) = w_0 + w_1(1-a) \quad (9)$$

by Chevallier and Polarski [3] (later popularized by Linder [4]) which does not suffer from that drawback and behaves nearly linear in  $z$  at low redshifts. (Clearly,  $w_0 = w(z=0)$  and  $w_1 = dw(z)/dz|_{z=0}$ ).

Now the dark energy density integrates to  $\rho_\phi = \rho_{\phi0} a^{-3(1+w_0+w_1+\epsilon)} \exp[3w_1(a-1)]$ . By contrast, the energy density of cold dark matter has no analytical expression but it can be found by numerical integration of Eq. (3.2). For the sake of illustration we present in Fig. 2 the evolution of its fractional density for a certain choice of parameters. Obviously, the expression for the baryon density does not vary.

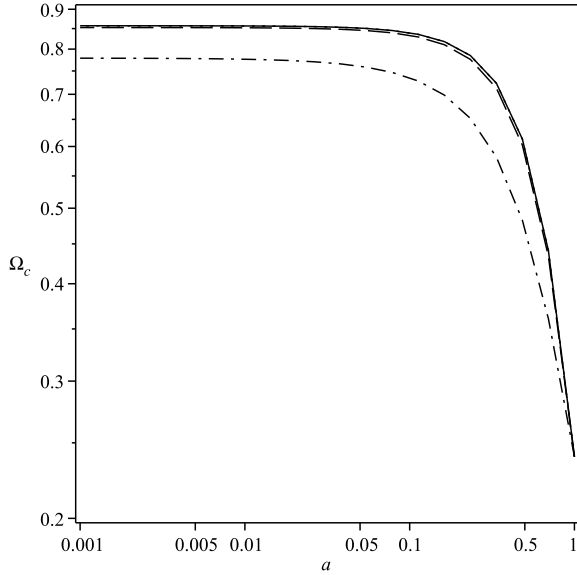


FIG. 2: Evolution of the fractional density of cold dark matter  $\Omega_c = \rho_c/(\rho_b + \rho_c + \rho_\phi)$ , since last scattering till now, in terms of the scale factor for the Chevallier-Polarski-Linder parametrization (9) with  $w_0 = -1$  and  $w_1 = 0.5$ . Solid, dotted, dashed, and dot-dashed lines correspond to  $\epsilon = 0, 10^{-4}, 10^{-2}$ , and  $0.1$ , respectively. The two first lines are undistinguishable from one another.

Proceeding as before, we numerically evaluate  $|\Delta\phi|/M_P$  in terms of the parameters  $\epsilon$ ,  $w_0$  and  $w_1$ . Figure 3 shows  $w_0$  vs.  $w_1$  for different choices of  $\epsilon$ . Points in the plane  $(w_1, w_0)$  satisfying simultaneously  $w_0 + w_1 > -1$  and  $w_0 > -1$  fulfill  $w(a) > -1$  for all  $a > 1$ -i.e., they correspond to quintessence models that never evolve into phantom. For small  $\epsilon$  condition (1) is violated in a section of the quintessence region, but only there. However, when  $\epsilon$  takes moderate values, the condition gets also violated by some models that evolved from phantom to quintessence (some few models in the mixed region I) and from some models that evolved in the opposite sense (some models in mixed region II), see right bottom panel. Models that always stay phantom respect condition (1) for all  $\epsilon$  at any redshift  $z \geq 0$ . The triangular region  $w_0 + w_1 > 0$  at the top right corner of each panel is observationally forbidden since points lying there correspond to models that feature dark energy dominance at high redshifts. It is noteworthy that it entirely falls in the region that violates condition (1). Likewise when  $\epsilon$  is about 0.029 or larger, an unphysical region of negative dark matter density develops -again in the region that violates (1)-, see right bottom panel. It is also visible that  $\Delta\phi$  slowly augments with  $\epsilon$ .

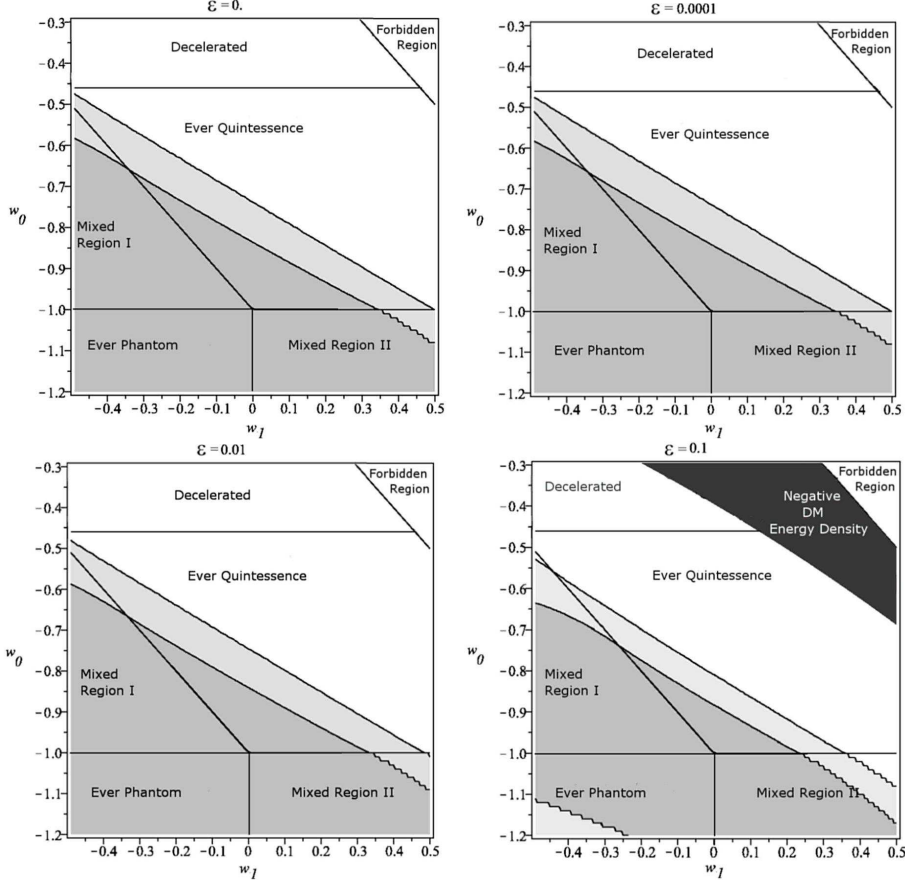


FIG. 3: In the light-gray sections of the four panels condition (1) is met when use of both (4.1) and the Chevallier-Polarski-Linder parametrization (9) is made. In the dark-gray sections,  $|\Delta\phi|/M_P < 0.7$ ; they shrink with increasing  $\epsilon$ . The regions marked ‘‘Ever Quintessence’’ correspond to models such that  $w_0 + w_1 > -1$  and  $w_0 > -1$  for all  $z > 0$ . Similarly, the regions marked ‘‘Ever Phantom’’ correspond to models such that  $w(a) < -1$  for all  $a < 1$ . In the mixed region I of each panel models transit from phantom to quintessence as the Universe expands. In the mixed region II they transit in the opposite sense. For  $w_0 > -0.46$  the expansion is decelerated at  $a = 1$ , as indicated in each panel, see the text.

Also marked in each panel is the maximum  $w_0$  for which there is acceleration at  $z = 0$ . This value,  $w_0 = -0.46$ , readily follows by setting the present deceleration parameter,  $q_0 = -\ddot{a}/(aH^2)|_{z=0} = \frac{1}{2}[1 + 3w_0(1 - \Omega_{b0} - \Omega_{c0})]$ , to zero.

As we have checked, for  $w$  values on the border of the forbidden region the ratio  $\Delta\phi/M_P$  is, at high redshifts (say,  $z > 20$ ), consistently larger than 2 and can be as large as 7 -see Fig. 4. The fact that  $w$  values in the forbidden region correspond to dark energy dominance

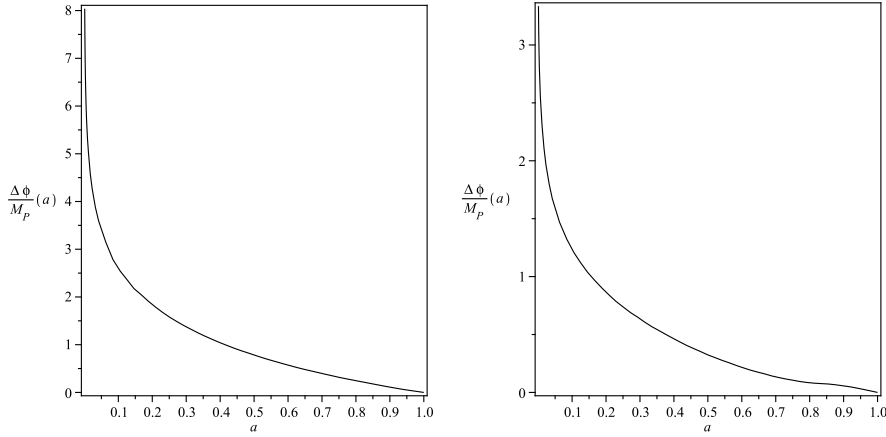


FIG. 4:  $\Delta\phi/M_P$  in terms of the normalized scale factor. In both panels  $\epsilon = 0.01$  and the  $w$  values correspond to points on the straight border line of the forbidden region of the left bottom panel of Fig. 3. Left panel:  $w_0 = -0.46$ . Right panel:  $w_0 = -1.2$ .

at early times and this is incompatible with observation (e.g., the primeval nucleosynthesis scenario and cosmic background radiation spectrum would be very different from the one admitted today, and galaxies could not have formed), suggests that, in general, scalar fields respect the bound (1). This also holds true for the forbidden regions of Figs. 6, 9, and 11 below.

### C. Barboza-Alcaniz parametrization

As readily noted, Chevallier-Polarski-Linder's parametrization (9) implies that  $w(z)$  diverges as  $z \rightarrow -1$  (i.e., in the far future). To avoid this unpleasant feature Barboza and Alcaniz proposed the ansatz  $w(z) = w_0 + w_1 \frac{z(1+z)}{1+z^2}$  or, equivalently,

$$w(a) = w_0 + w_1 \frac{1-a}{1-2a+2a^2}, \quad (10)$$

which ensures that  $w(z)$  stays bounded in the whole interval  $-1 \leq z < \infty$  aside from behaving linearly in redshift for  $|z| \ll 1$  [22].

Assuming this novel parametrization alongside the interaction term (4.1), we get  $\rho_\phi = \rho_{\phi 0} a^{-3(1+w_0+w_1+\epsilon)} (1-2a+2a^2)^{3w_1/2}$ . Again,  $\rho_c$  must be calculated numerically. Figure 5 illustrates the behavior of  $\Omega_c$ .

Proceeding as before, we numerically assess  $|\Delta\phi|/M_P$  in the redshift interval  $(0, z_{ls})$ . Figure 6 depicts  $w_0$  vs.  $w_1$  for various choices of  $\epsilon$ . If  $w_1 > 0$ , quintessence models lie in the

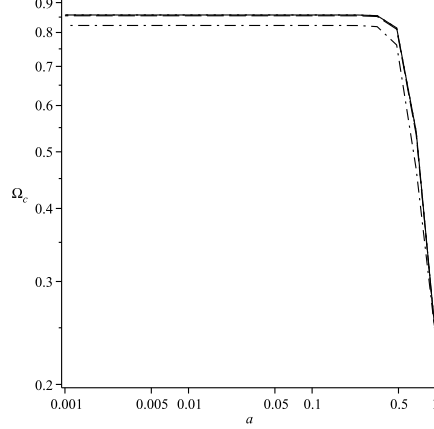


FIG. 5: Evolution of the fractional density of cold dark matter  $\Omega_c = \rho_c/(\rho_b + \rho_c + \rho_\phi)$  in terms of the normalized scale factor using the parametrization of  $w(a)$  of Barboza and Alcaniz (10) with  $w_0 = -1$  and  $w_1 = -1.5$ . Solid, dotted, dashed, and dot-dashed lines correspond to  $\epsilon = 0, 10^{-4}, 10^{-2}$ , and  $0.1$ , respectively; the three first practically overlap each other.

region given by  $-1 \leq w_0 - 0.21 w_1$  and  $w_0 + 1.21 w_1 \leq 1$ ; if  $w_1 < 0$ , they lie in the region  $-1 \leq w_0 + 1.21 w_1$  and  $w_0 - 0.21 w_1 \leq 1$ . Unlike the preceding section, in the mixed regions II of the parameter space, phantom models (that started as quintessence at high redshift) violate condition (1) for whatever  $\epsilon$ . As before, the triangular regions given by  $w_0 + w_1 > 0$  are observationally discarded as they correspond to dark energy dominance at early times. These ones are much wider than in the previous case. Again a region of negative cold dark matter density develops, this time for  $\epsilon$  values in excess of 0.015 -see right bottom panel. As it is apparent, the interaction has a noticeably effect on the variation of  $\phi$  in the sense that  $\Delta\phi$  moderately augments with  $\epsilon$ . Comparison of Figs. 3 and 6 reveals that the interaction induces a bigger evolution of  $\phi$  when  $w(z)$  follows Barboza-Alcaniz's parametrization than when it follows the parametrization of Chevallier-Polarski-Linder.

### III. INTERACTION TERM PROPORTIONAL TO THE COLD DARK MATTER DENSITY

In this section we take up  $Q = 3\epsilon H\rho_c$  for the coupling term and resort to the expressions for the equation of state parameter considered in the previous section.

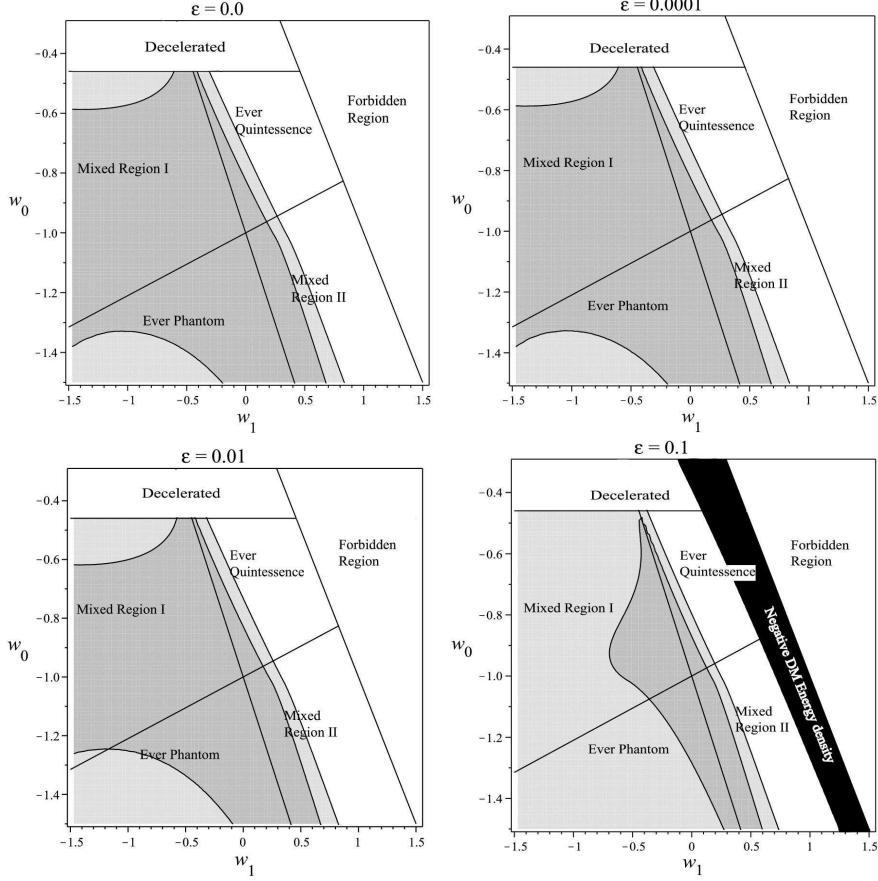


FIG. 6: Same as in Fig. 3 except that  $w(a)$  obeys the parametrization of Barboza and Alcaniz, Eq. (10).

### A. Constant $w$

For  $w = w_0$  we readily find

$$\begin{aligned} \rho_c &= \rho_{c0} a^{-3(1-\epsilon)}, \\ \rho_\phi &= \rho_{\phi0} a^{-3(1+w_0)} + \rho_{c0} \frac{\epsilon}{w_0 + \epsilon} [a^{-3(1+w_0)} - a^{-3(1-\epsilon)}]. \end{aligned} \quad (11)$$

Fig. 7 shows  $|\Delta\phi|/M_P$  vs.  $w_0$  for different values of  $\epsilon$ . For quintessence fields there is a range of  $w_0$  that violates condition (1) regardless the value of  $\epsilon$ . For phantom fields the said condition only holds when  $\epsilon$  is very small. This contrast with non-interacting phantom models which fulfill  $|\Delta\phi|/M_P < 1$  irrespective of  $w_0$  (see Fig.1 of Ref. [2]).

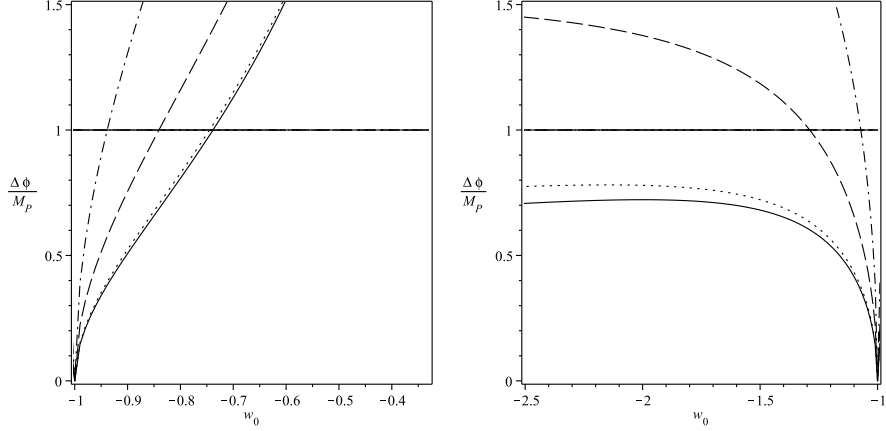


FIG. 7:  $|\Delta\phi|/M_P$  vs.  $w_0$  for  $Q$  given by (4.2) and constant  $w$  evaluated in the redshift range  $(0, 1089)$ . Left Panel: Quintessence solutions  $(-1 < w_0 < -1/3)$ . Right panel: Phantom solutions  $(w_0 < -1)$ . In both panels solid, dotted, dashed, and dot-dashed lines correspond to  $\epsilon = 0, 10^{-4}, 10^{-2}$ , and  $0.1$ , respectively. Condition (1) implies  $w_0 < -0.738$  for  $\epsilon = 0$  and  $w_0 < -0.745$  for  $\epsilon = 10^{-4}$ ; for  $\epsilon = 10^{-2}$  it implies  $-1.299 < w_0 < -0.841$ , and  $-1.071 < w_0 < -0.939$  for  $\epsilon = 0.1$ .

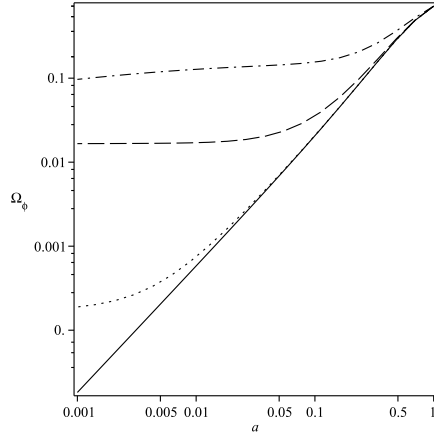


FIG. 8: Evolution of the fractional density of dark energy for the Chevallier-Polarski-Linder parametrization, Eq. (9), with  $w_0 = -1$  and  $w_1 = 0.5$ . Solid, dotted, dashed, and dot-dashed lines correspond to  $\epsilon = 0, 10^{-4}, 10^{-2}$ , and  $0.1$ , respectively.

### B. Chevallier-Polarski-Linder parametrization

In this case  $\rho_c = \rho_{c0} a^{-3(1-\epsilon)}$  while the expression for  $\rho_\phi$  must be found numerically. Figure 8 instances the evolution of  $\Omega_\phi$  in terms of the normalized scale factor.

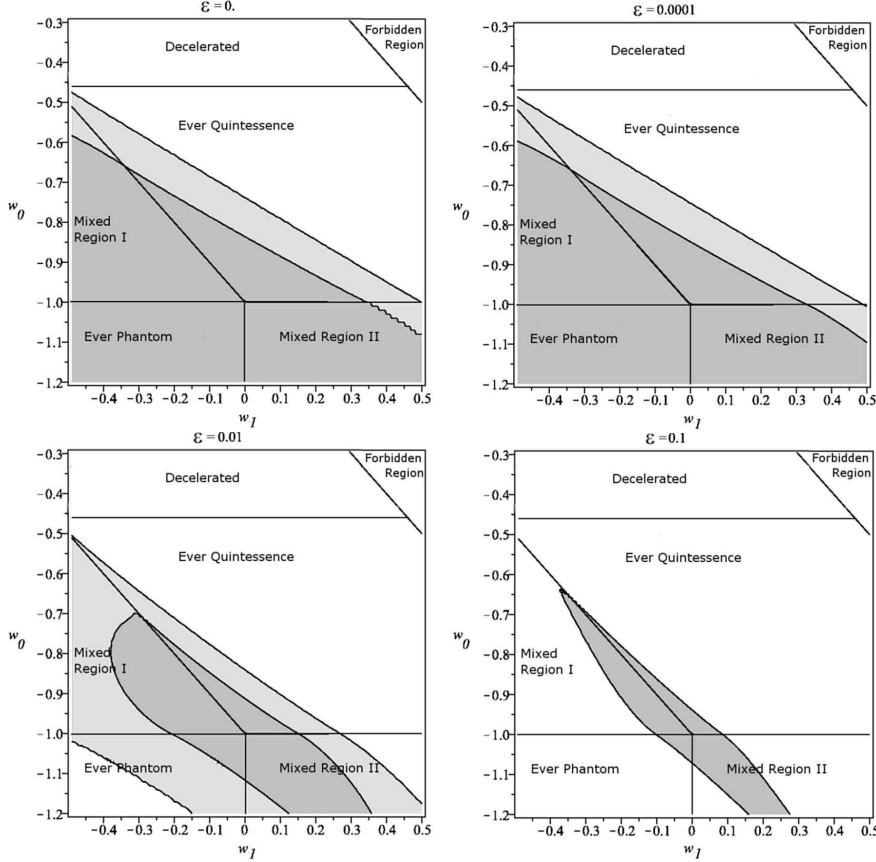


FIG. 9: Same as Fig. 3 except that the interaction term is now given by Eq. (4.2) and that in the right bottom panel only the  $|\Delta\phi|/M_P < 1$  region is depicted.

Dark energy models in Fig. 9 such that  $w_0 + w_1 > -1$  and  $w_0 > -1$  present a quintessence behavior during its whole evolution. For small  $\epsilon$  only models in this region can violate condition (1). For larger  $\epsilon$  values, models in the other regions (bottom panels) can also violate it. As it is manifest, the area of the offending region augments with  $\epsilon$ . As in the preceding cases, models in the upper right triangle of each panel are observationally discarded.

### C. Barboza-Alcaniz parametrization

In this instance  $\rho_c$  bears the same expression in terms of the scale factor than in the previous case. Figure 10 illustrates the dependence of  $\Omega_\phi$  on  $a$ .

After having numerically evaluated  $|\Delta\phi|/M_P$ , Fig. 11 displays  $w_0$  vs.  $w_1$  for different choices of  $\epsilon$  in the redshift interval  $(0, z_{ls})$ . If  $w_1 > 0$ , ever quintessence models belong to

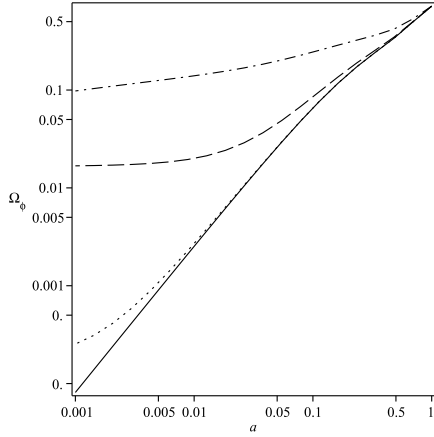


FIG. 10: Evolution of the fractional density of dark energy for the Barboza-Alcaniz parametrization, Eq. (10), with  $w_0 = -1$  and  $w_1 = 0.5$ . Solid, dotted, dashed, and dot-dashed lines correspond to  $\epsilon = 0, 10^{-4}, 10^{-2}$ , and  $0.1$ , respectively.

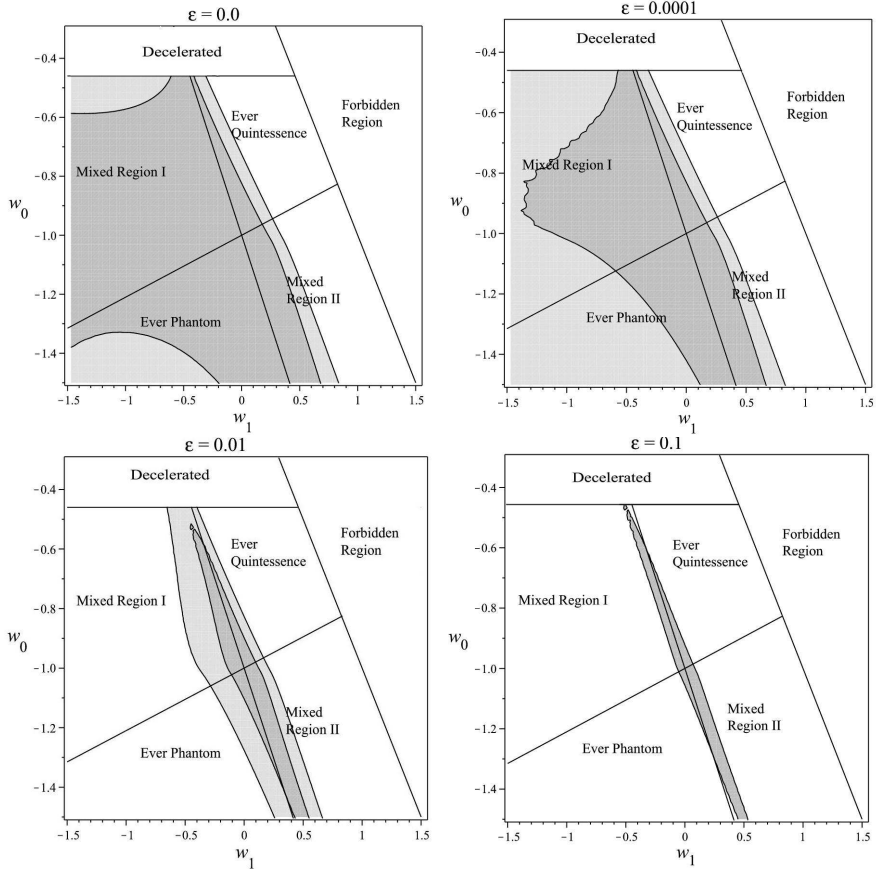


FIG. 11: Same as in Fig. 9 except that  $w(a)$  obeys the parametrization of Barboza and Alcaniz, Eq. (10).

the region given by  $-1 \leq w_0 - 0.21w_1$  and  $w_0 + 1.21w_1 \leq 1$ ; if  $w_1 < 0$ , they lie in the region  $-1 \leq w_0 + 1.21w_1$  and  $w_0 - 0.21w_1 \leq 1$ . Even for small  $\epsilon$ , models in this region as well as models in the mixed region II can breach condition (1) (top panels). For larger  $\epsilon$  values, models in the other regions (bottom panels) can also breach it. As it is apparent from the right bottom panel ( $\epsilon = 0.1$ ), models that always stay phantom are restricted to a very narrow region close to the line  $w_0 = -1 - 1.21w_1$ .

#### IV. DISCUSSION

Motivated by the reasonable assumption that the variation  $\Delta\phi$  of the field driving the present phase of cosmic accelerated expansion should not exceed Planck's mass we have numerically calculated the said evolution since last scattering till now for different expressions of the equation of state parameter  $w(a)$  and two couplings,  $Q$ , between dark matter and dark energy. This constrains the parameter space  $(w_1, w_0)$  as shown in the six cases studied. Figures 1, 3, 6, 7, 9, and 11 explicitly exhibit the regions of the parameter space  $(w_1, w_0)$  that fulfill the bound  $|\Delta\phi|/M_P < 1$ . Our analysis extends those of Huang [1] and Saridakis [2] who assumed that dark matter and dark energy evolved separately and did not consider Barboza and Alcaniz's parametrization [22].

The main results of this work can be summarized as follows:

- (i) When the interaction obeys (4.1), models that always stay phantom respect condition (1) at any redshift and for any  $\epsilon$  value. (ii) Likewise, depending on the values taken by  $w_0$  and  $w_1$  models that always stay as quintessence as well as models that evolve from quintessence to phantom and models that evolve in the opposite sense can violate the said condition. (iii) When  $Q$  obeys (4.2) and  $w(a)$  is given by the Chevallier-Polarski-Linder parametrization (9), for small  $\epsilon$ , all models that ever stay phantom and all models in the mixed regions I and II respect bound (1); -top panels of Figs. 9. However, for not so small  $\epsilon$  values, models in these regions may also violate (1) -bottom panels of Fig. 9. (iv) When  $Q$  is given by (4.2) and  $w(a)$  obeys the Barboza-Alcaniz parametrization (10), for small  $\epsilon$ , all models that ever stay phantom and models in the mixed region I satisfy bound (1) -top panels of Fig. 11. By contrast, for not so small  $\epsilon$  values, models in these regions may also violate (1) -bottom panels of Fig. 11. (v) The dark energy field  $\phi$  appears to evolve faster when: (a) the coupling  $Q$  depends explicitly on  $\rho_c$  than when it does on  $\rho_\phi$ , and (b) when  $w(a)$

obeys the parametrization of Barboza-Alcaniz than when it does that of Chevallier-Polarski-Linder. Point (a) is in line with Caldera-Cabral *et al.* result that interacting models with  $Q = 3\epsilon H\rho_\phi$  “work better” than models with  $Q = 3\epsilon H\rho_c$  [16]. Further, these models may help explain the non-vanishing temperature (about 0.6 Kelvin [23]) of sterile neutrinos [24].

Our finding that  $|\Delta\phi|$  increases with  $\epsilon$  strengthens the view expressed in the Introduction that  $Q$  must be small. Otherwise (except for (4.1) and  $w = \text{constant} < -1$ , right panel of Fig. 1) condition (1) would be violated for whatever  $w$  not far from  $-1$ .

We have confined ourselves to models in which the interaction term is proportional to the Hubble factor (Eqs. (4)) whence our results apply to them only. Other interaction terms can be found in the literature, among others,  $Q \propto \dot{\phi}\rho_c$  [25], and  $Q \propto (\rho_c + \rho_\phi)$  -see e.g. [16, 26]. However, the former class of models present the drawback of being unable to simultaneous lead to a correct sequence of cosmic eras (radiation, matter, and dark energy) and solve the coincidence problem [27], while the models we have considered do not suffer from that [28]. As for the latter class of models, they generally lead to negative energy densities, either of dark matter or dark energy, at early or late times [26]. Still, for some specific values of the parameters entering the interaction these models are free of that problem.

As is well known, due to quantum instabilities phantom fields may find no place in Nature -see e.g. [29]. However, some phantom models based on low-energy effective string theory may not suffer from such pathologies [30] whence this issue is not settled as yet. Moreover, higher derivative terms in the Lagrangian may render phantom models stable [31].

Before closing, it is sobering to recall that variable dark energy fields are afflicted by the problem of their small mass ( $m_\phi \sim 10^{-33}$  eV). Due to this unpleasant feature they are looked upon as not more natural than the cosmological constant, despite the enormous fine tuning scale of the latter. Admittedly, this is an unsolved problem that affects most (if not all) candidates of evolving dark energy. However, recently, a supergravity based approach that might point to the solution has been proposed [32]. It provides a very small mass for the field and a seemingly natural mechanism for a weak coupling between the field and matter.

## Acknowledgments

G.I. research was funded by the “Conseil Régional de la Bourgogne”. This work has been partly supported by the Spanish Ministry of Science and Innovation under Grant FIS2009-

13370-C02-01, and the “Direcció de Recerca de la Generalitat” under Grant 2009SGR-00164.

---

- [1] Q.-G. Huang, Phys. Rev. D **77**, 103518 (2008).
- [2] E. N. Saridakis, Phys. Lett. B **676**, 7 (2009).
- [3] M. Chevallier and D. Polarski, Int. J. Mod. Phys. D **10**, 213 (2001).
- [4] E.V. Linder, Phys. Rev. Lett. **90**, 091301 (2003).
- [5] T. Banks, M. Dine, P.J. Fox, and E. Gorbatov, JCAP 06(2003)001.
- [6] Q.G. Huang, Phys. Rev. D **76**, 061303(R) (2007).
- [7] X.-M Chen, J. Liu, and Y-G. Gong, Chin. Phys. Lett **25**, 8 (2008).
- [8] R. Bean, S.H. Hansen, and A. Melchiorri, Phys. Rev. D **64**, 103508 (2001).
- [9] P.J.E. Peebles and B. Ratra, Rev. Mod. Phys. **75**, 559 (2003); K. Hagiwara *et al.*, Phys. Rev. D **66**, 010001(2002).
- [10] P.J. Steinhardt, in *Critical Problems in Physics*, edited by V.L. Fitch and D.R. Marlow (Princeton University Press, Princeton, 1997).
- [11] S. del Campo, R. Herrera, and D. Pavón, Phys. Rev. D **78**, 021302(R) (2008); *ibid* JCAP 01(2009) 020.
- [12] E. Abdalla, *et al.*, Phys. Lett. B **673**, 107 (2009).
- [13] M. Hicken *et al.*, Astrophys. J. **700**, 331 (2009).
- [14] A. Shafieloo, V. Sahni, and A.A. Starobinsky, Phys. Rev. D **80**, 101301(R) (2009).
- [15] C. Wetterich, Nucl.Phys. B **302**, 668 (1988); W. Zimdahl, D. Pavón, and L.P. Chimento, Phys. Lett. B **521**, 133 (2001); L. Amendola and D. Tocchini-Valentini, Phys. Rev. D **66**, 043528 (2002); G. Farrar and P.J.E. Peebles, Astrophys. J **604**, 1 (2004); G. Olivares, F. Atrio-Barandela, and D. Pavón, Phys. Rev. D **71**, 063523 (2005); H. Zhang and Z.-H. Zhu, Phys. Rev. D **73**, 043518 (2006); S. del Campo, R. Herrera, and D. Pavón, Phys. Rev. D **74**, 023501 (2006); R. Manini and S. Bonometto, JCAP 06(2007)020; Z.-K. Guo, N. Ohta, and S. Tsujikawa, Phys. Rev. D. **76**, 023508 (2007); J.H. He and B. Wang, JCAP 06(2008)010; T. Koivisto, and D. Mota, Astrophys. J. **679**, 1 (2008); X. Fu, H. Yu, and P. Wu, Phys. Rev. D **78**, 063001 (2008); P.M. Sutter and P.M. Ricker, Astrophys. J. **687**, 7 (2008); J. Valiviita, E. Majerotto, and R. Maartens, JCAP 07(2008)020; J.-H. He, B. Wang, and E. Abdalla, Phys. Lett. B **671**, 139 (2009); J.-H. He, B. Wang, and Y.P. Jing, JCAP 07 (2009) 030.

- [16] G. Garcia-Cabral, R. Maartens, and L.A. Ureña-López, Phys. Rev. D. **79**, 063518 (2009).
- [17] F. Atrio-Barandela and D. Pavón, “Interacting dark energy” in *Dark Energy-Current Advances and Ideas*, edited by J.R. Choi (Research Signpost, Trivandrum, Kerala, India; in press, 2010).
- [18] D. Pavón and B. Wang, Gen. Relativ. Grav. **41**, 1 (2009).
- [19] N. Kaloper and K.A. Olive, Phys. Rev. D **57**, 811 (1998).
- [20] R. Curbelo, T. González, G. León, and I. Quirós, Class. Quantum Grav. **23**, 1585 (2006).
- [21] H. Zhang and Z.-H. Zhu, Phys. Rev. D **73**, 043518 (2006).
- [22] E.M. Barboza Jr. and J.S. Alcaniz, Phys. Lett. B **666**, 415 (2008).
- [23] S.H. Hansen, J. Lesgourgues, S. Pastor, and J. Silk, Mon. Not. R. Astr. Soc. **333**, 544 (2002).
- [24] J. Zhou, B. Wang, D. Pavón, and E. Abdalla, Mod. Phys. Lett. A **21**, 1689 (2009).
- [25] See, e.g., third paper in [15].
- [26] G. Caldera-Cabral, R. Maartens, and B.M. Schaefer, JCAP 07(2009)027.
- [27] L. Amendola, M. Quartin, and S. Tsujikawa, Phys. Rev. D **74**, 023525 (2006).
- [28] G. Olivares, F. Atrio-Barandela, and D. Pavón, Phys. Rev. D **77**, 063513 (2008).
- [29] J.M. Cline, S.-Y. Jeon, and G.D. Moore, Phys. Rev. D **70**, 043543 (2004).
- [30] F. Piazza and S. Tsujikawa, JCAP 07(2004)004.
- [31] P. Creminelli, G. D’Amico, J. Noreña, and F. Vernizzi, JCAP 02(2009)018.
- [32] P. Brax, C. vand de Bruck, J. Martin, and A.-C. Davis, JCAP 09(2009)032.